

# Chapter 6

## Intravascular Ultrasound Tissue Characterization Analysis

The goal of automatic tissue characterization is to identify the different kind plaques in IVUS images. This process requires two tasks: identification of what the plaque is and labelling of the different areas of the plaque. Figure 6.1 illustrates roughly the procedure of supervised tissue characterization. The IVUS image 6.1.a is preprocessed and sent to the automatic tissue characterization system. Figure 6.1.c shows the first step, the accurate location of the lumen-plaque border and the adventitia border. Between both lies the plaque, which is the region of interest to be classified. Figure 6.1.d exemplifies the tissue characterization process. We are focussed on the plaque, and try to find and label areas corresponding to different plaques. In the figure, light gray areas are soft plaque, white areas are fibrotic plaque and dark gray areas are calcium plaque. At the end of the process we obtain the tissue characterized IVUS (figure 6.1.e) to be used by the physicians. These results have been used to validate against the manually segmented plaque regions (figure 6.1.b).

This chapter illustrates the work in IVUS image analysis and tissue characterization. The layout of the chapter is the following: The first section is concerned with plaque discrimination. This means that our goal is to find the characteristic structures in the IVUS images in order to obtain an accurate approximation of the location of the plaque. The second section shows the complexity of the problem of tissue characterization from the point of view of a classical classification and describes a full framework for IVUS analysis.

### 6.1 IVUS structure analysis

The main structures in IVUS images are two: The first one is the *intima border*. The intima border is the line that separates the blood pool (also known as *lumen*) and the tissue. This border is usually well defined in IVUS images since it is an abrupt transition from erratic small structures (representing the blood) and well defined and high-echoreflexive elongated structures (usually plaque and artery wall). An example of this structure is shown in figure 6.2. The other important structure is the

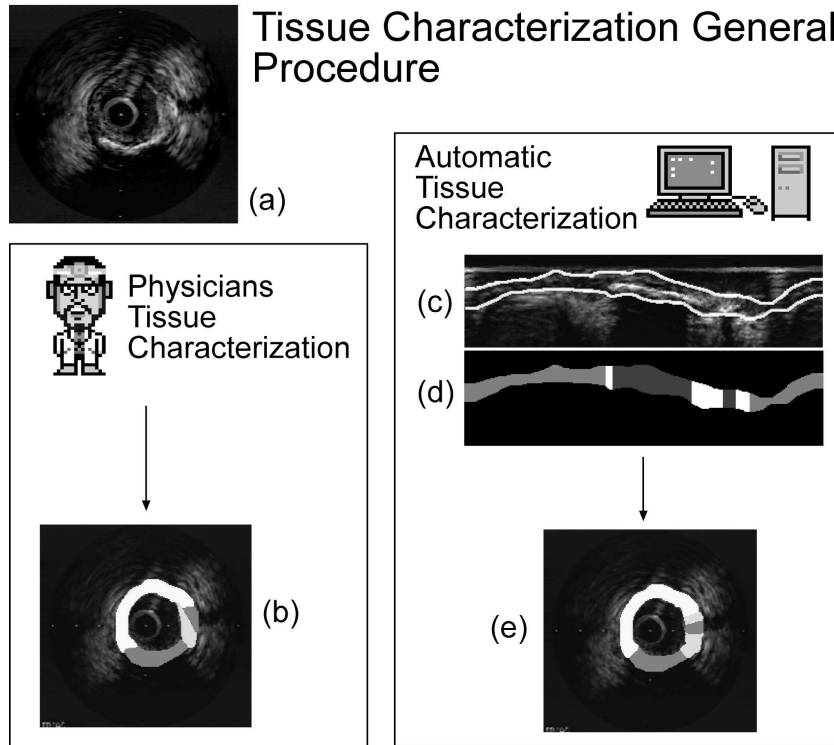


**Figure 6.1:** The tissue characterization process can be done manually by physicians (a)-(b) or by an automatic process (a)-(c)-(d)-(e). (c) Segmentation of the lumen-plaque border and adventitia border. (d) Pre-processed image of the plaque characterization. (e) Final IVUS tissue characterization.

*adventitia border.* The adventitia border defines the separation between deposited materials (such as fibrous, lipidic or calcium sediments) and the artery wall. Figure 6.2 shows an example of this structure. Our goal is to find an accurate location of both since, the area between both is what we know as *plaque*.

The segmentation of the plaque is a really important step before tissue characterization, as has been shown in [43] [44] [45] [19] [20].

The main reference in IVUS structure analysis is Sonka et al. [43]. In the paper, the process of segmentation relies on a manual definition of a region of interest. Using that region of interest a Sobel-like edge operator with neighborhoods of  $5 \times 5$  and  $7 \times 7$  is applied. Once we have these features extracted, the problem of identification of the vessel wall and plaque border is solved by finding the optimal path in a two-dimensional graph. The key of the graph searching is to find the appropriate cost functions. In the paper, the author proposes different cost functions depending on whether the lumen-plaque border or the adventitia border is desired.

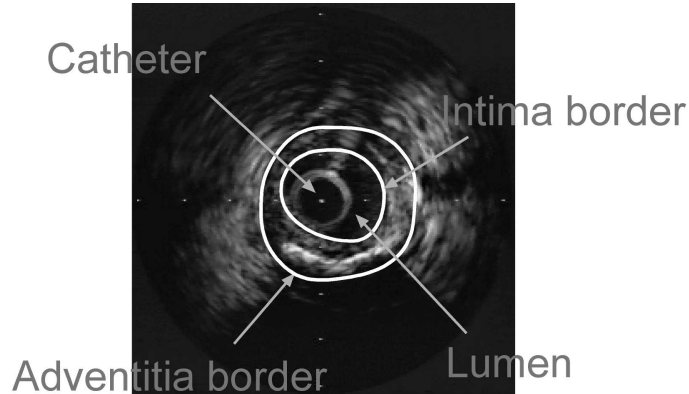


**Figure 6.2:** Characteristic structures in IVUS images.

### 6.1.1 Segmentation of the plaque (I): Intima segmentation

Having in mind the tissue classification goal of the process, [19] [20] try to find a segmentation of the the lumen-plaque border as well as to find an overall approximation to the tissue area independent of what kind tissue it is. The method consists on selecting a suitable feature space and a classifier. We have focussed our work in texture feature spaces since the same feature space can be used later for particular tissue discrimination in the plaque area. Thus, the first step is to train a classifier for general tissue discrimination.

The classification step is performed using a fast classifier, either boosting methods or maximum likelihood classification. The result of this step is a series of unconnected areas that are related to tissues. In order to find the exact location of the lumen-plaque border, a fast parametric snake is let to deform over the unrelated areas.[46] The snake performs a double task: first, it finds a continuous boundary between blood and plaque. The second task is that it ensures an interpolation and a fill-in process in regions where tissue is not located or not reliable (such as areas with reverberations due to the guide-wire, etc). The intima border detection process described in the former lines is illustrated in figure 6.3.

To validate our approach we have used 10 sequences from 3 different patients. The training step has been done using 4 sequences of 2 patients (different from the validation patients). We have used the following feature spaces:

- Scale-space Filter Bank (Derivatives of Gaussian). The scale parameter varies with the following values:  $\sigma = 0.5, 1, 2, 4, 8$ . For each scale, a set of directional derivatives is extracted. Particularly, this set is  $\partial^n = [\partial_0, \partial_{90}, \partial_0^2, \partial_{60}^2, \partial_{120}^2, \partial_0^3, \partial_{45}^3, \partial_{90}^3, \partial_{135}^3]$ , where the subindex points the direction of the partial derivative in degrees.
- Co-occurrence matrices measures. The measures have been obtained using a quantization in 256 gray levels, neighborhoods of  $N=(5,8)$  pixels of radius and relative distance between the center of the neighborhood and the computed

## Methodology:

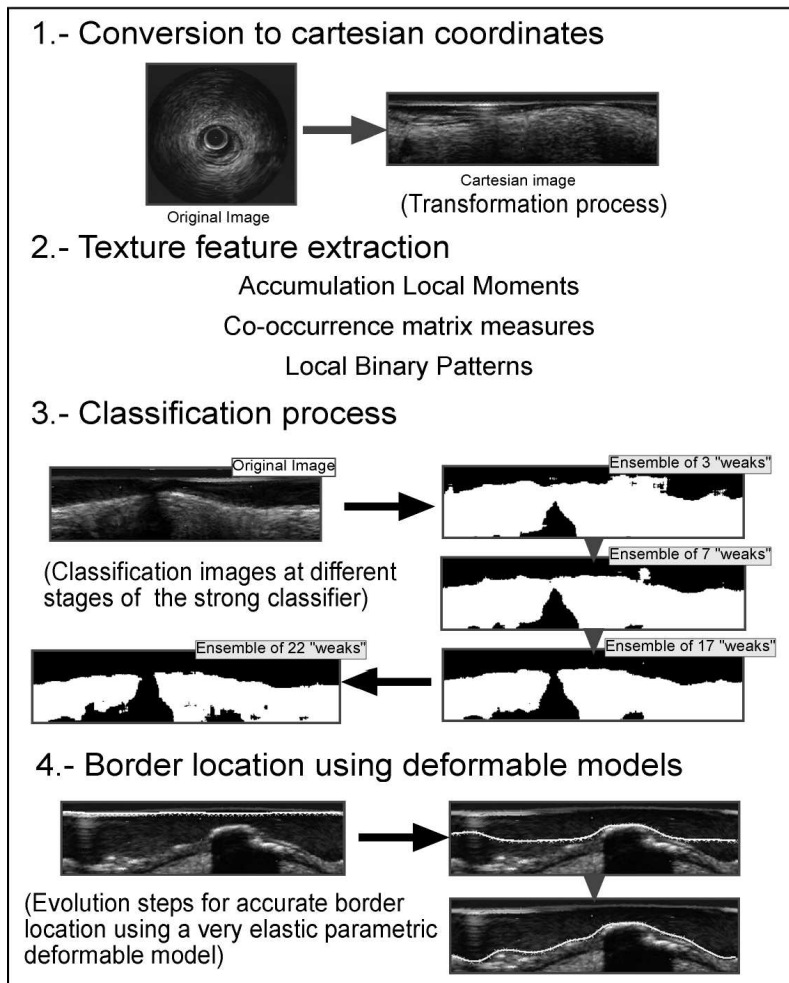


Figure 6.3: Tissue classification.

Feature space	Mean Error	Maximum Error
Co-occurrence measures	$0.24 \pm 0.04$	$0.61 \pm 0.10$
Wavelets	$0.66 \pm 0.09$	$1.34 \pm 0.13$
Derivative of Gaussian	$0.17 \pm 0.03$	$0.60 \pm 0.13$
Cumulative moments	$0.17 \pm 0.04$	$0.43 \pm 0.09$
Local Binary Patterns	$0.08 \pm 0.06$	$0.35 \pm 0.10$

**Table 6.1:** Maximum and mean errors of each of the methods in mm.

pixel of  $D=(2,3)$ . We have also used four orientations for creating each matrix at each distance and each neighborhood radius.

- Wavelets Family. Different experiments with these features pointed out the best performance in our problem of biorthonormal 1.5 with neighborhood radius of  $N=9$  pixels.
- Cumulative moments up to degree  $(k,l) = (9,9)$  have been used in neighborhoods of  $N=(3,5)$
- Local Binary Patterns have been used with neighborhoods of  $N=\{1,2,3\}$  different radius.

Table 6.1 shows the maximum and mean errors (in millimeters) of the performance of our method when compared to physicians manual segmentation. The comparison have been done computing the relative distance in millimeters between each of the points of the physicians segmentation to the boundaries provided by our segmentation.

In the table we can see that Local Binary Patterns feature space with maximum likelihood has the best performance with a really low error rate. These results improve the reported intima border detection rates in literature up to date. It must be noted

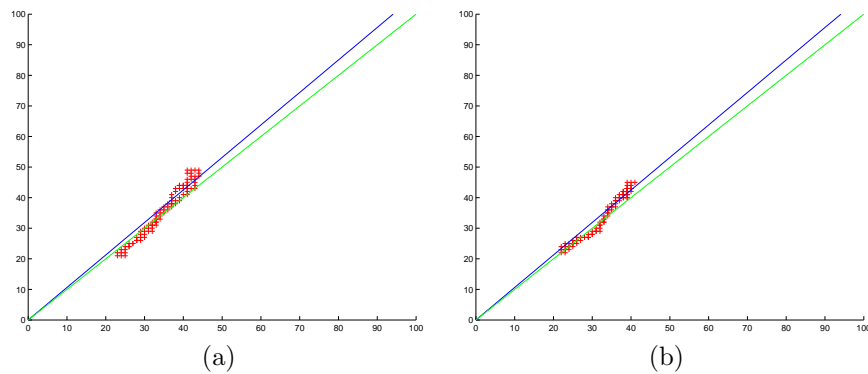


**Figure 6.4:** Regression line for two different patients. Abscise shows the automatic positioning of the borderline. Ordinate shows the physicians positioning of the borderline.

that the error measures are greatly hurt by bad classification results originated if we are unable to remove all the artifacts effects (such as guide-wire reflections, or echoes from the catheter wrapping). Some methods are more sensitive to this kind of artifacts than others. This fact is observed comparing cumulative moments with scale-space filter banks and co-occurrence matrix measures. Cumulative moments show more robustness to artifacts than the other methods, this fact is enhanced by the help of the needed post-processing step due to the random noise of the classification results when using this method. However, when the image is free from artifacts these three methods perform similar. We must note that the method is fully automatic once the texture model is build. The snake parameters used are  $\alpha = 0.3$  and  $\beta = 0.3$ ; these weights stands for the parameters associated to tension and rigidity respectively. We have used a cubic B-Spline implementation of snakes. The area operators remove thin lines with horizontal orientation and speckle noise of less than 5 pixels of area.

Figure 6.4 show two regression lines comparing the accuracy of physicians location of the intima border and the automatic location for the same border using local binary patterns. As can be seen the correlation coefficient,  $r$ , is over 0.96.

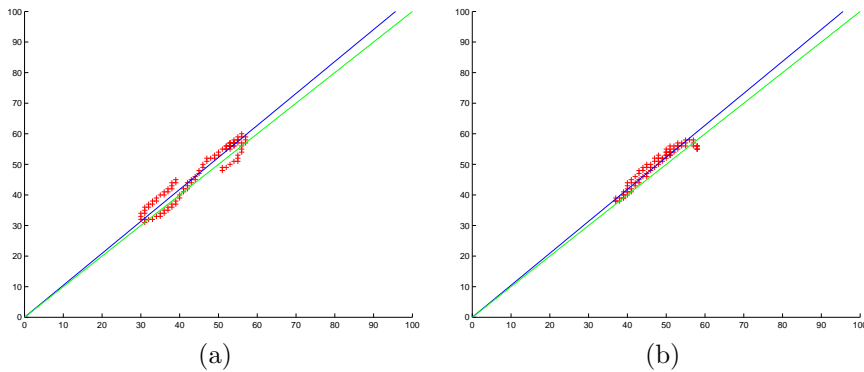


**Figure 6.5:** Regression line for the adventitia border location of two different patients. Abscise shows the automatic positioning of the borderline. Ordinate shows the physicians positioning of the borderline.

### 6.1.2 Segmentation of the plaque (II): Adventitia segmentation

The problem of adventitia segmentation is one of the most difficult problems when dealing with IVUS images, and still remains open for the scientific community. However, in order to have an approximation of the adventitia location we propose to use contextual information once the intima has been found.

The first step in our approach is to define the most likely area for the adventitia to be found. In order to do this we reuse the tissue classification obtained in the intima segmentation process. This segmentation defines the whole tissue area in the IVUS image, and therefore, can be used to define a external borderline to delimit the adventitia search procedure. We use a deformable model to find the external

	Mean error	Max error	Regression val	Median
Error (mm.)	$0.20 \pm 0.14$	0.68	0.937	0.14

**Table 6.2:** Error rate in millimeters of the adventitia location compared with physicians segmentation.

borderline of the tissue.

The approximation we propose uses a  $5 \times 5$  Sobel-like operator over a smoothed version of the IVUS image. The borders found using the former filter are cleaned. A certain value is given to each border according to the likelihood of being adventitia. This value is purely empirical and based on context. After that we let a deformable model adapt to the features extracted. This snake is initialized between the intima and the external tissue border.

Figure 6.5 show two regression lines comparing the accuracy of physicians location of the adventitia border and the automatic location for the same border using our scheme. As we can observe there is a really good correlation between the physicians segmentation and the automatic segmentation.

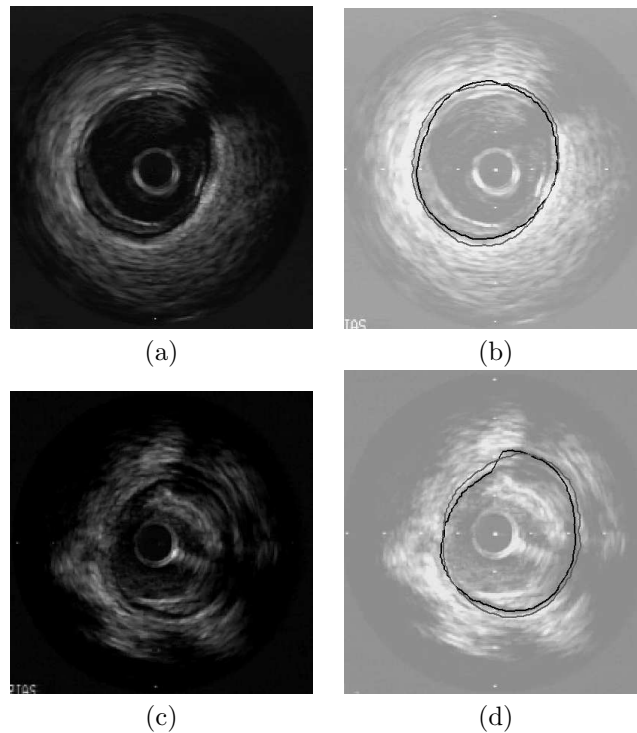


**Figure 6.6:** Examples of the adventitia segmentation. In dark gray a physician segmentation. In black automatic segmentation. (a) Original image. (b) Automatic segmentation of (a). (c) Original Image. (d) Automatic segmentation of (c).

Table 6.2 shows the mean, maximum and median error rates of the methodology used to locate the adventitia border. Though the figures show a good behavior of the method (the mean error of 0.2 mm. correspond to 5 pixels of the image) it must be further improved to reduce false positive adventitia locations. In this sense, working in a third dimension would be profitable since false positives due to spurious structures would not have continuity and therefore would be distinguishable from the adventitia border.

Figure 6.6 shows two examples of the adventitia location. Figures 6.6.a and 6.6.c are the original images, while figures 6.6.b and 6.6.d are the comparison between the automatic segmentation (displayed in black) and the physicians segmentation (in dark gray).

## 6.2 Tissue characterization

This section is divided in two different subsections. The first one is concerned with the problem of tissue characterization in a general framework. An objective database using physicians categorization of isolated tissues has been built and used for general analysis of the textural features discrimination using a boosting framework. The second subsection describes the final methodology used for plaque characterization in non-isolated regions (we exploit tissue correlation between adjacent regions) taking into account also computational time issues.

### 6.2.1 Pairwise general texture-based tissue discrimination

The assessment of pairwise plaque classification process is presented in this section. First, the database building and experimental settings are introduced. Then, a discrimination classification reference for methodology comparison is shown. After the reference, we are explaining the multiple pair-wise problems and the results of their classification. We finish this section showing the characteristic curves of the behavior of the AdaBoost process.

#### Experimental settings and database building

One of the main problems in the IVUS scientific community is the lack of a standard reference set for validation of the IVUS tissue classification. Regarding this matter, we have devoted a great amount of time in collaboration with expert physicians to create a database with ten thousand samples of each of the four tissues acknowledged by experts, soft tissue, fibrous tissue, mixed tissue and calcium. Those samples have been extracted from 20 different patients, using a *Clearview* device from Boston Scientifics Corp. and a 40 MHz *Atlantis* catheter. Using this database, several texture descriptors have been selected.

Particularly, we have chosen

- Derivatives of gaussian filter bank, up to the third derivative. A five level multi-resolution framework is used, with scales  $\{0.2, 0.5, 1, 2, 4\}$ . For each scale, a set of directional derivatives is extracted. Particularly, this set is  $\partial^n =$



Feature Set	Computational Complexity	Discriminative Power
Filter bank	High	High
Co-occurrence set	High	High
LBP	Low	High
Cumulative Moments	Low	Average

**Table 6.3:** Computational complexity and performance for each set.

$[\partial_0, \partial_{90}, \partial_0^2, \partial_{60}^2, \partial_{120}^2, \partial_0^3, \partial_{45}^3, \partial_{90}^3, \partial_{135}^3]$ , where the subindex points the direction of the partial derivative in degrees. To this set we also include the zero-derivative image, that is a smoothed version at the corresponding level of the original image.

- A set of descriptors of the co-occurrence matrices at angles  $\{0, 45, 90, 135\}$  with neighborhoods of  $11 \times 11$  pixels and distance for the co-occurrence pair of  $D = 2$  and a  $17 \times 17$  pixels neighborhood with a distance of  $D = 3$ .
- A tissue description set based on local binary patterns and local variance, using radius 1 with 8 samples, radius 2 with 16 samples and radius 3 with 24 samples.
- A feature space based on cumulative moments, with moments up to  $(9, 9)$ .

All these feature spaces are well-known and well-suited spaces for texture description. They usually differ from each other in terms of computational complexity and discriminative power. Table 6.3 shows the performance of each feature set. Note that the filter bank and co-occurrence matrix descriptors approach have high discriminative power and high computational complexity. On the other hand, local binary patterns and cumulative moments are fast but their discriminative power is lower.

Regarding the Adaboost procedure, we use a composition of 500 classifiers in the original feature space for each description set.

### Discrimination Reference

To compare the performance of the boosting method we have selected a well-known classifier, Fisher Linear Discriminant Analysis. The results of this classifier are our ground-truth, to which we refer in order to compare the results of the Adaboost technique.

Plaque pair	BOF	COOC25	COOC38	LBP	MOM
Fibrous vs Calcium	35.18%	24.55%	23.84%	48.53%	46.43%
Soft vs Calcium	25.30%	10.07%	9.94%	42.97%	44.10%
Mixed vs Calcium	29.64%	18.51%	17.83%	46.55%	46.14%
Soft vs Fibrous	34.83%	35.81%	34.57%	48.46%	47.67%
Fibrous vs Mixed	44.56%	47.68%	49.84%	49.91%	49.70%
Soft vs Mixed	42.73%	40.30%	49.36%	46.94%	47.87%

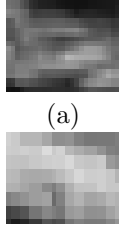
**Table 6.4:** Error rate for each plaque pair, using the different tissue descriptors.

Table 6.4 shows the test error rate for each pair of plaques. Having a look at the figures, the table reveals that there are some sets with a great amount of overlapping samples. This is particularly true in the discrimination between mixed tissue and soft or fibrous tissue, since mixed tissue implies an ill-defined mixture of both fibrous and soft tissues. We can also see that some feature spaces tend to perform better for our problem than others. In fact, co-occurrence matrices descriptors (COOC25, COOC38) and derivatives of gaussian filter bank (BOF), outperform clearly the low complexity descriptors, Local Binary Patterns (LBP) and cumulative MOMents (MOM). This means that both feature spaces, describe better the tissue properties than the other two families of descriptors. However, this fact could have been easily predicted from table 6.3, since there is always a trade-off between complexity and performance.

### The Fibrous vs Calcium problem

The characterization of the calcium tissue seems to be the less difficult one since the calcium tissue has a very high echo-reflectivity and homogeneity. On the other hand, fibrous plaque is also high reflective, but have much more rugosity.

Feature Set	Initial Error	Final Error
BOF	33.13%	13.09%
COOC25	20.90%	13.74%
COOC38	20.67%	11.04%
LBP	24.76%	21.81%
MOM	43.62%	38.04%



(a)

(b)

**Figure 6.7:** Examples of the fibrous tissue (a) and the calcium plaque (b).

Figure 6.7 shows an example of the fibrous plaque (fig.6.7.a) and the calcium plaque (fig.6.7.b) . The table from figure 6.7 shows the results for this test. As expected the initial error in the overall feature space of the best performing sets and the error using discriminant analysis are quite close to each other. However, the Adaboost procedure refines the classification thus increasing the recognition rates to an average of 88%. Unexpectedly, LBP has a relative good performance, close to 80%, making it an ideal candidate if we aim for fast processing.

### The Soft vs Calcium problem

This problem is by far the most simple one since the plaques we are distinguishing are the more different kind of plaques. In particular, the soft tissue has low echo-reflectivity and high granularity, while the calcium plaque is just the opposite.

Figure 6.8 shows an example of the fibrous plaque (fig.6.8.a) and the calcium plaque (fig.6.8.b) . The former statement is confirmed by the table shown in figure 6.8, that shows the figures for the error rate in this problem. Again, the recognition rate of the high complexity spaces is pretty high, and further increased by the AdaBoost process, up to an average over 95%. Three important remarks can be made looking

Feature Set	Initial Error	Final Error
BOF	17.75%	5.80%
COOC25	9.81%	7.27%
COOC38	8.88%	4.29%
LBP	15.31%	14.68%
MOM	45.49%	33.00%

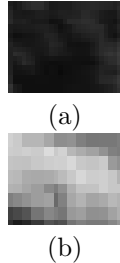


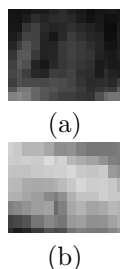
**Figure 6.8:** Examples of the soft tissue (a) and the calcium plaque (b).

at the figures. First, there is a huge improvement in performance using derivatives of gaussian, of about 12%. Second, LBP still has pretty good results: over 85%. Third, and the most surprising, MOM still performs bad in this stage. Looking at the reference table 6.4 we can see that there is a huge improvement in LBP performance and BOF performance. LBP lowers its error rate by 30% and BOF lowers its error rate by 20%.

### The Mixed vs Calcium problem

Since the behavior of the soft and fibrous plaque against calcium tissue is fairly good, we expect this problem to be an "average" of the above ones.

Feature Set	Initial Error	Final Error
BOF	26.29%	9.79%
COOC25	16.36%	12.44%
COOC38	15.91%	7.46%
LBP	20.54%	19.15%
MOM	44.16%	35.75%



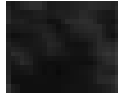
**Figure 6.9:** Examples of the mixed tissue (a) and the calcium plaque (b).

Figure 6.9 shows an example of the mixed plaque (fig.6.9.a) and the calcium plaque (fig.6.9.b). Certainly, this is what happens, the results are not as good as the soft versus calcium problem, (see table in figure 6.9) but are better than the fibrous versus calcium one. This is logical if we recall that the mixed tissue is a combination of both fibrous tissue and lipid tissue in an interleaved way. At this stage, we have clearly a good vision of what is the performance of each feature space as well as the influence of the adaboost process in the problem. BOF and COOC38 performs the best after adaboost, granting high recognition rates. COOC25 seems to perform the worst of the trio formed by the high complexity classifiers. If we compare this results to the ones obtained using FLD, BOF lowers its error rate by 20%, and COOC38 by 10%.

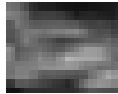
### The Soft vs Fibrous problem

One of the most interesting and less obvious problems is the soft vs fibrous problem. In this case, both plaques have a good amount of texture involved in them (high granularity), although, there is a difference in the reflectivity of the transducer pulse.

Feature Set	Initial Error	Final Error
BOF	28.63%	26.41%
COOC25	27.58%	27.53%
COOC38	26.57%	25.98%
LBP	31.62%	30.93%
MOM	44.41%	38.43%



(a)



(b)


**Figure 6.10:** Examples of the soft tissue (a) and the fibrous plaque (b).

Figure 6.10 shows an example of soft plaque (fig.6.10.a) and fibrous plaque (fig.6.10.b). Table in figure 6.10 shows the performance of the AdaBoost procedure when applied to this problem. We can conclude from the figures, that in this case, the AdaBoost process does not help much. This fact, seems to show that the way data is distributed in the feature spaces is clearly entwined. This fact hinders the process of the combination of classifiers, since, presumably, each weak classifier is focusing on a really low amount of misclassified data. In this case, the comparison of the results with the reference of Fisher, improves the recognition rate by 10%.

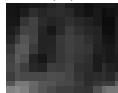
### The Fibrous vs Mixed problem

This problem and the soft vs mixed problems are by far the most complex ones. The fibrous and the mixed plaques really resemble each other in terms of local distribution features. The difference between both is simply the spatial overall distribution of the tissues. Most of the methods we have tried are purely local, and therefore are destined to fail in this problem. In fact, we have seen that the mixed label is also the most disagreed of the plaques among the experts labelling. However, we also attach the results for these two problems.

Feature Set	Initial Error	Final Error
BOF	37.74%	36.28%
COOC25	39.99%	37.33%
COOC38	39.40%	35.65%
LBP	41.31%	40.90%
MOM	43.42%	40.92%



(a)



(b)

**Figure 6.11:** Examples of fibrous tissue (a) and mixed plaque (b).

Figure 6.11 shows an example of fibrous plaque (fig.6.11.a) and mixed plaque (fig.6.11.b). Table in figure 6.11 shows the error rates for this problem.

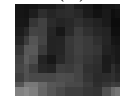
### The Soft vs Mixed problem

In the same way than the former case, the soft versus mixed plaque problem is ill-posed from the local texture point of view.

Feature Set	Initial Error	Final Error
BOF	40.44%	37.36%
COOC25	37.72%	33.09%
COOC38	35.42%	29.29%
LBP	39.35%	39.01%
MOM	46.45%	41.26%



(a)



(b)

**Figure 6.12:** Examples of the soft tissue (a) and the mixed plaque (b).

Figure 6.11 shows an example of soft plaque (fig.6.11.a) and mixed plaque (fig.6.11.b). Table in figure 6.12 shows the results for this case. It is remarkable the fact that COOC38 is able to distinguish both plaques with an average recognition rate of over 70%. This is due to the fact that COOC38 use a  $17 \times 17$  neighborhood and therefore is susceptible to pick up the spatial distribution of the entwined fibrous and soft plaques.

The fibrous vs. mixed and soft vs. mixed using linear discriminant analysis can not be made, since the results show that the decision is nearly random (recognition rates of about 55%). However, using AdaBoost the problem seems to have a weak solution, that is, a solution of nearly 70% of recognition. This is quite evident as mixed plaque is formed by mixing soft and fibrous plaques.

### Characteristic curves

As stated in the AdaBoost description section, the error rate of the weak classifiers increases at each iteration (every time we add a classifier) due to the fact that it has to classify the previously erroneous classified data (the errors of the combination of weak classifiers up to this moment). The other characteristic of this process is that the overall error rate on the training data tends to zero as the number of weak classifiers increases. This fact does not imply that the test classification error also tends to zero. In fact, it has been shown, and we will see in the figures, that it can worsens or keep nearly constant.

Figure 6.13 shows some examples of the characteristic behavior of the AdaBoost process. Figures 6.13.a and 6.13.b refer to the behavior of the derivatives of gaussian in front of the soft-calcium and mixed-calcium problems respectively. Figure 6.13.c shows the error curves for the accumulation moments in front of the fibrous-calcium problem. Figure 6.13.d shows the aforementioned constant behavior of the test error

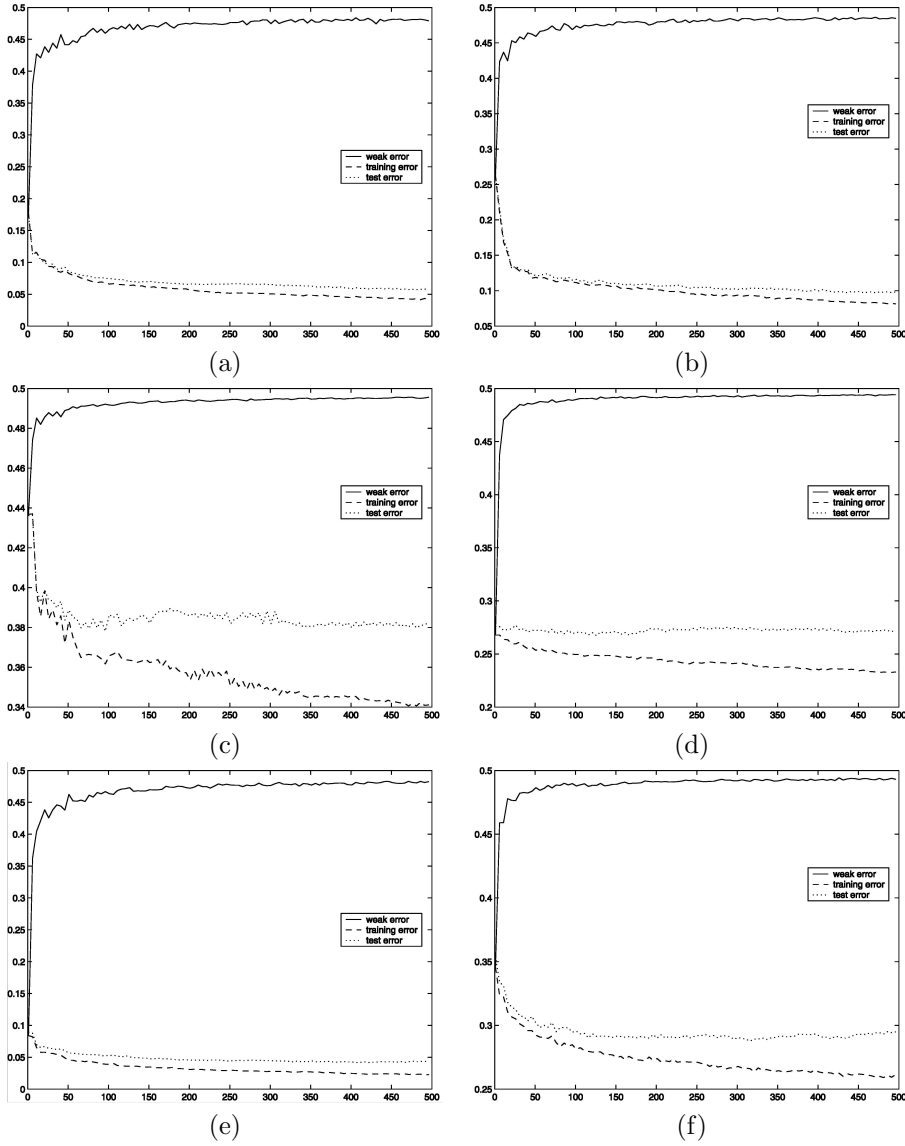


**Figure 6.13:** Examples of the characteristic curves for the AdaBoost process. (a) BOF in soft-calcium problem. (b) BOF in mixed-calcium problem. (c) MOM in fibrous-calcium problem. (d) COOC25 in soft-fibrous problem. (e) COOC38 in soft-calcium problem. (f) COOC38 in soft-mixed problem.

rate although the training error rate clearly decreases. This figure refers to the co-occurrence (2, 5) when characterizing soft versus fibrous plaque. Figures 6.13.e and 6.13.f show co-occurrence matrix descriptors for parameters (3, 8) in front of the problems soft-calcium and soft-mixed plaque, respectively.

### Full classification using pairwise discrimination

From the classified tissue pairs we can use a *winner takes all* approach for full classification performance. This approach classifies the plaque according to the majority of votes for each pair. In our experiments there has been no draw instances.

Method	Soft RR	Fibrous RR	Calcium RR	Error
COOC38	74.15%	59.20%	85.79%	23.85%
COOC25	72.51%	58.16%	85.68%	27.88%
BOF	75.15%	59.68%	84.38%	29.04%
LBP	73.03%	47.63%	71.48%	35.62%
MOM	43.06%	41.28%	51.26%	52.98%

**Table 6.5:** Recognition rate for each method and mean error using pairwise classification.

Table 6.5 shows the recognition rate using this approach, as well as the mean error derived from this method. As we have observed in the single pairs, the tendency of the performance using each feature space remains the same. Co-occurrence matrix measures outperforms the rest of the methodologies. We can argue that the lack of good results using cumulative moments and local binary patterns comes from the small spatial support they use to extract the features. In summary, the results seem to point out that high performance is related to the size of the neighboring area used to extract texture features.

### Discussion

The first conclusion that arises from the experiments is the beneficial influence that the AdaBoost procedure has in the classification of the plaque, thus, rendering it to a very good classifier if we aim for plaque characterization.

Regarding the feature spaces, co-occurrence matrices descriptors performs better than the rest, closely followed by the bank of filters approach. Local binary patterns is the third in recognition rate.

Several aspects have to be taken into account when judging the results. First of all, regarding the database: the data included in the database is widely variable representing different plaque appearance by different patients cases. Analyzing the plaques, we saw that different plaques from different patients can be quite different among each other, although they are grouped under the same label. It is surprising how some plaques labelled as different can resemble to each other. This fact also seems to point out that more information must be taken into account when dealing with plaque characterization. We observed that physicians heavily rely on the context information, and the location of the plaque. Therefore, the results presented here are

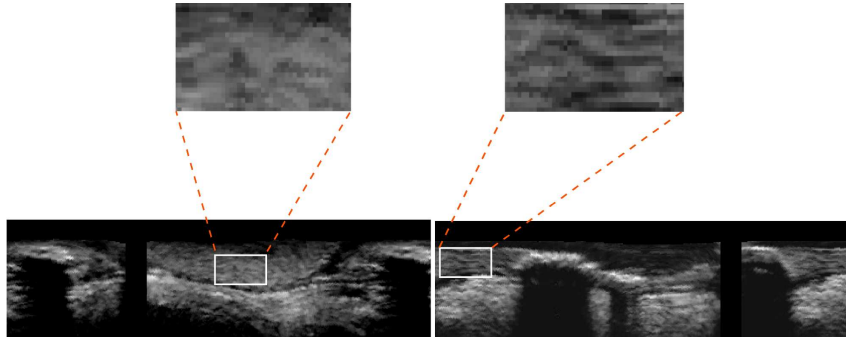


**Figure 6.14:** Illustration of how the local classification of tissue can be deceiving.

useful as a guideline of the performance of the classifiers but they are by no means a criterion to avoid the less accurate feature descriptors.

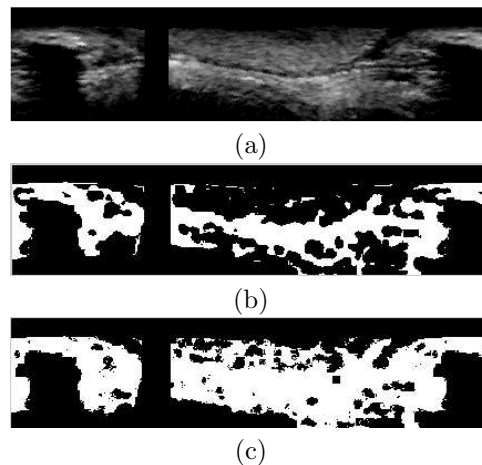


**Figure 6.15:** Adaboost overtraining and fake-plaque effect. a) Original image b) 50 classifiers c) 500 classifiers

In particular, we can see from the study that MOM based classifiers lead to low recognition rates. While it provides not so good results as a feature space, we have seen that using contextual information most of the misclassified data can be seen as speckle noise caused by the decision of the classifier. That means that in the context of an IVUS image, the misclassified data points are scattered and can be re-classified taking into account neighboring plaques, since more of them are in isolated groups of two or three pixels. If this is done, accurate results can be extracted from them. This reinforces the idea shown at the previous paragraph, the analysis of the contextual information can easily improve the recognition rate of the methods.

Figure 6.14 shows an example of how the local information can not be enough for a good classification. In fact, if we look at the top images, we can see that both



images are quite similar and we probably will classify them as some kind of plaque, in particular as fibrous plaque. However if we look at the original images we can see that one is in fact a tissue plaque, but the other it is not a tissue, it is part of the blood pool (lumen), although with very similar appearance.

The effect of the previous casuistic can lead to undesirable situations such as the one showed in figure 6.15. This figure is a simplification of the tissue problem. In particular, this is a blood versus tissue classification, but it will serve to easily understand some concepts. The figure is an example of two effects. On one hand, the final recognition rate is low because of the fake-plaque effect, as mentioned in the former paragraph. On the other hand, this is a classical example of an overtrained classifier. Figure 6.15.b shows the classifier results in a middle stage of learning. Figure 6.15.c shows the final result. As we can see, as the blood is relatively different from the blood expected, and because the last group of classifiers added in the AdaBoost process are more focused on very few samples of the training data, they can degrade the final classification result if the particularities of the training data do not coincide with the ones of the test set.

In summary, AdaBoost is a very high performance classifier, the results show that plaque characterization based only on texture can not be made accurately if we want recognition rates over 85%. Furthermore, the most different kind of tissue, calcium is easily identified even without context information, with an overall accuracy of over 95%. However, mixed plaques are really difficult to distinguish. This points out that if we want to classify mixed plaques texture descriptors alone are not suitable for the task.

The "fake-plaque" effect opens the possibility to create a new kind of classification process that takes into account the particular test set to infer context information and therefore adapt the classification process to the particularities of the test set.

## 6.2.2 Full framework for Tissue characterization

Despite the results using the database for non-contextual aided tissue characterization, we have deepened in the identification of the different kind of plaques by developing a strategy for fast and accurate automatic plaque recognition using information from the whole image.

We begin the process of tissue characterization taking the IVUS image and transforming it to cartesian coordinates (figure 6.16.a). Once the cartesian transformation is done, artifacts are removed from the image (figure 6.16.b). There are three main artifacts in an IVUS image: the transducer wrapping, that creates a first halo at the center of the image (in the cartesian image the echo is shown at the top of the image); the guide-wire effect, that produces an echo reverberation near the transducer wrapping; and the calibration grid, which are markers at a fixed location that allow the physicians to evaluate quantitatively the morphology and the lesions in the vessel. With the artifacts removed, we proceed to identify intima and adventitia using the process described in the former section. At this point, we have the plaque located and we are concerned with tissue identification (figure 6.16.c). The tissue classification process is divided in three stages: First, the soft-hard classification (figure 6.16.d and figure 6.16.e), in which the soft plaque, the hard plaque and calcium are separated.

Feature space	Qualitative speed	Qualitative performance
Co-occurrence measures	Slow	Good
Gabor space	Slow	Acceptable
Wavelets	Fast	Poor
Derivative of Gaussian	Slow	Acceptable
Cumulative moments	Fast	Good
Local Binary Patterns	Fast	Good

**Table 6.6:** Descriptive table of the discriminative power of each feature space using k-nearest neighbors.

In the second stage, the calcium is separated from the hard plaque (figure 6.16.f and figure 6.16.g). At the last stage, the information is fused and the characterization is completed. We will refer later to this diagram to explain some parts of the process.

Recall that the plaque is the area comprised between the intima and the adventitia. With both borders located we can focus in the tissue of that area. For such task, a three stages scheme is used. First, a classification of the soft plaque is performed. This process discriminates between soft plaque and the rest, fibrotic plaque and calcium. The second stage, is the identification of calcium based on finding shadowed areas after the plaque. The last stage is the integration of all the information to produce the final characterization.

To evaluate the results, a classification of over 200 full-tissue regions from 20 different patients has been performed. The training set is a subset of two thirds of the overall data determined using bootstrapping strategy. The rest of the data has been used as test set. Previously, different physicians have determined and delineated plaque regions in each full-tissue image.

Regarding the first stage of the process, a classification is performed on the feature space. At this point, a feature space and a classifier must be selected. To help to chose which feature space and which classifier to use, we try each of the feature spaces with a general purpose classifier, the k-nearest neighbors method. Regardless the classifier used, the information provided at the output of the system is a raw classification. Using these data we can further process it to obtain clear borders of the soft and the mixed plaques.

Figure 6.17 shows the performance of K-NN method applied to several feature spaces. Observing the images, we realize that scale-space processes, DOGs, Gabor filters and wavelets, have poor to acceptable discrimination power, and therefore are not suitable for the task of tissue discrimination. On the other hand, statistic-based feature spaces and structure feature spaces have acceptable to good performances. The following table 6.6 details the conclusions arisen from the experiment. The qualitative speed nomenclature (fast/slow) indicates the viability of the feature space technique to be included in a real time or near-real time process. Note that the images displayed are pixel-based classification results and have no further "cleaning" processing.

Up to this point we have worked with raw classification data, which is sensible to classification noise. Therefore a "cleaning" procedure can be used to incorporate local spatial information in the classification process. Different processes can be applied to achieve this goal, two possible approaches are region based area filtering and

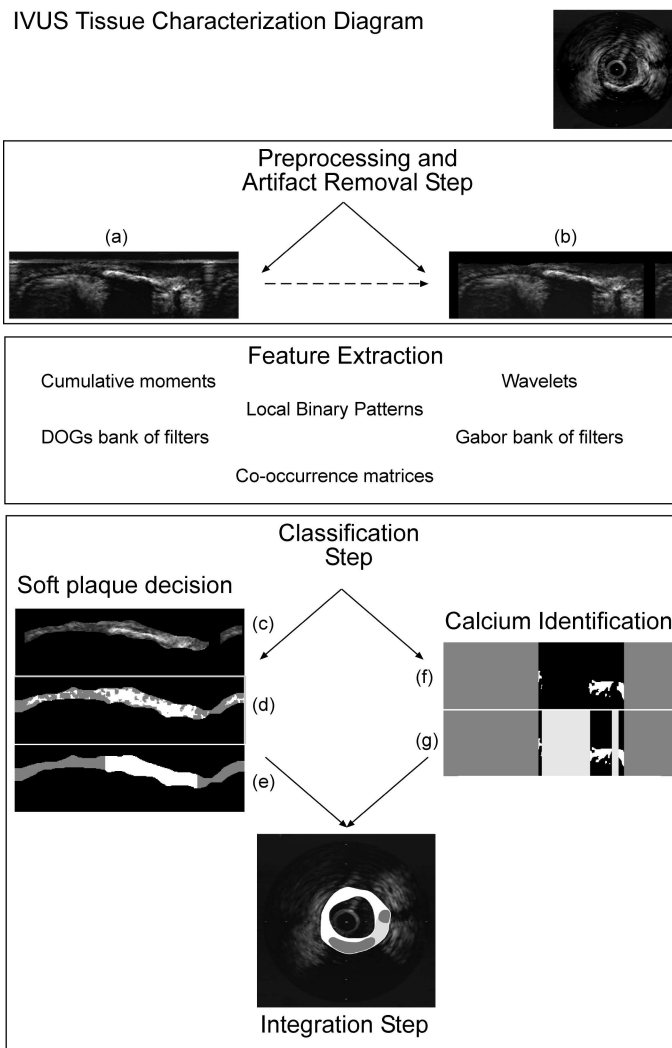
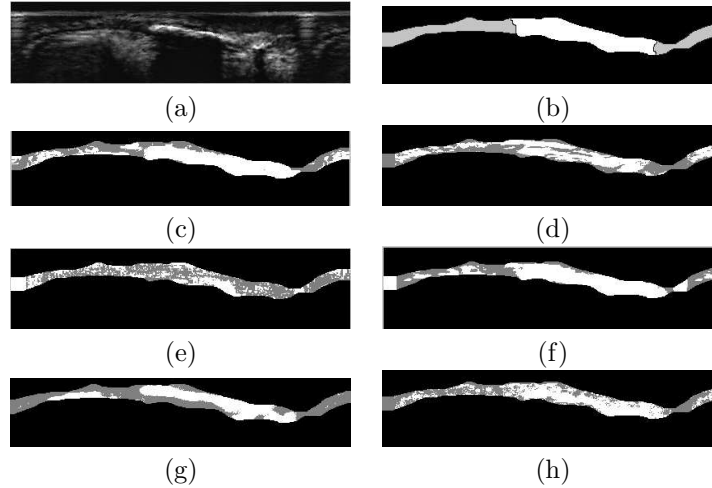


Figure 6.16: Tissue characterization diagram



**Figure 6.17:** Tissue raw classification data using 7-Nearest Neighbors. (a) Original image in cartesian coordinates. (b) Expert manual classification of tissue. (c) Co-occurrence feature space. (d) Gabor feature space. (e) Wavelets feature space. (f) Derivative of Gaussian feature space. (g) Cumulative Moments feature space. (h) Local Binary Patterns feature space.

classification by density filtering. In a region based area filtering the less significant regions in terms of size are removed from the classification. On the other hand, the other method relies on keeping the regions that have high density of classification responses. As the classification exclusively aims to distinguish between soft and hard plaque, a separate module is added to separate hard plaque from calcium.

Table 6.7 and table 6.8 show the error rates for RAW data (**RAW Error**) and Post-processed data taking into account neighboring information and density of responses (**Post Error**). It is also shown the percentages of false positives (**FP**) and false negatives (**FN**) for both errors. The false positives and false negatives are included as they gives information of the possible geometry of the samples in the feature space.

The result of the classification of the test data using all feature spaces and 7- nearest neighbors classifier is shown in table 6.7. Observing the RAW data error rate, the best overall feature spaces are co-occurrence matrix, local binary patterns, derivatives of gaussian and accumulation local moments. These results are confirmed looking at the post-processing error rate and ratifies the qualitative evaluation shown in table 6.6, where we observe that the same feature spaces are the ones that perform best. Analyzing each of the feature spaces in terms of false positive and false negative rates, we can deduce that: Co-occurrence feature space has good discrimination power, having a "symmetric" nature that is both FP and FN rates are comparable. In the same sense, we can deduce that the overlapping of both classes is similar. Derivatives of gaussian's filter space has tendency to over-classify hard plaque. The classes in the feature space are not very well defined as hard-plaque must have a higher scatter than the soft-plaque. Gabor filter's bank gives a good description of both classes

Feature space	RAW Error	FP	FN	Post Error	FP	FN
Co-occurrence	22.36	10.91	11.45	10.88	4.19	6.68
DOG	27.81	23.51	4.95	16.29	16.67	0.04
Gabor	35.26	18.86	17.22	16.26	16.49	0.07
Wavelets	45.05	20.52	24.90	31.78	24.40	7.68
Moments	31.72	16.42	15.30	12.17	11.36	0.81
LBP	25.67	9.67	16.23	3.45	2.67	0.81

**Table 6.7:** Feature space performance using K-Nearest Neighbor.

Feature space	RAW Error	FP	FN	Post Error	FP	FN
Co-occurrence	40.88	34.66	6.20	12.91	12.10	0.81
Moments	35.50	20.34	16.16	13.83	13.02	0.81
LBP	26.37	5.76	20.85	6.93	1.52	5.47

**Table 6.8:** Feature space performance using ML and FLD if necessary.

as they have similar false rates. However, both classes are very overlapped giving a hard time to the classification process. Wavelets overlapping of classes in the feature space is extremely high, therefore it describes bad each of the classes. Accumulation local moments have similar description power than Gabor filter's bank, however the different responses from both allow a much better post-processing in Accumulation Local Moments. This fact allows us to suppose that the classification error points in the image domain are much more scattered and with very few local density. Local Binary Patterns have good descriptive power as well as giving a more sparse pattern in false positives and negatives in the image domain.

To further develop our discussion we will only take the three best post-processed data performing feature spaces: Co-occurrence matrix measures, Accumulation Local Moments and Local Binary Patterns. Up to this point we have neither taken into account complexity of the methods nor time issues. However, these are critical parameters in real applications, thus, we considerate them in our following discussions.

Once the feature space is selected, the next decision is to find the most suitable classifier taking into account our problem constraints, if any. If we are concerned with speed issues, simple but powerful classifiers are required. Due to the high dimensionality of two of the feature spaces selected (co-occurrence matrix measures have about 24 features per distance and accumulation local moments have 81 features) a dimensionality reduction step is desired. Principal component analysis is the first obvious choice, but due to the great amount of overlapping data the results are worse than using Fisher's linear discriminant analysis which is focalized in finding the most discriminative axes for our given set of data.

The result of this experiment is shown in table 6.8. We use Maximum Likelihood combined with a Fisher Linear Discriminant Analysis reduction. As Local Binary Patterns do not need dimensionality reduction due to the small amount of features computed (3 features), the comparison with this method is done by just classifying with the maximum likelihood method. As expected, the raw results are much worse with this kind of classifier. COM measures take the worse part doubling its error

Ensemble num.	RAW Error	FP	FN	Post Error	FP	FN
Base error	34.86	28.20	6.98	41.94	40.33	1.10
Ensemble of 5 c.	29.38	16.32	13.32	33.17	31.87	1.10
Ensemble of 10 c.	31.44	7.36	23.37	13.92	5.22	7.76

**Table 6.9:** Error rates using boosting methods with ML with the accumulation local moments space.

ratio. However, LBP, though it has also worse error ratio with ML, manages to be the most discriminative of the three methods. This fact is also shown in the post-processing, where LBP still have the lower error ratio. COM measures regain their discrimination power after the post-processing.

Therefore, using one of the fastest classifiers, maximum likelihood, one achieve a classification ratio over 87%. If the selected feature space is LBP, the scheme is the fastest possible scheme as LBP are computationally efficient and low time consuming as well as the ML classifier is without dimensionality reduction. This scheme is really well suited for real-time or near-real-time applications due to both time efficiency and reliability in the classification. This is, however, by no means the only near-real-time configuration available since accumulative local moments are computationally as fast as local binary patterns. However, the FLD dimensionality reduction hinders the process. To overcome this problem, other classifiers can be used. The necessity to find reliable and fast classifiers lead us to boosting techniques.

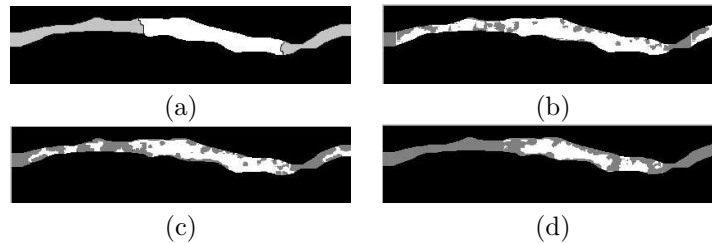


**Figure 6.18:** Boosting procedure for tissue characterization at different stages of its progress. (a) Expected hand classification by an expert. (b) First stage of the boosting procedure. (c) Ensemble of five classifiers classification. (d) Ensemble of ten classifiers classification.

Boosting techniques allow a fast and simple classification procedure to improve its performance as well as maintaining part of its speed. To illustrate this fact figure 6.18 shows the evolution of the classification when more classifiers are added to the *strong classifier*.

The error rates at different stages of the process are also shown in table 6.9. These results are computed using a ML method as a *weak classifier* on the ALM space. The numbers show how the error rate is improving, and, though the raw classification error rate is nearly immutable, we can observe that there is a great change in the classification data points distribution in the image domain since the false positive and negative rates drastically change. The post processing error rate

gives better description of what is happening. The disposition of the error points in the classification image is more sparse and unrelated to their neighborhood, allowing better post processing and classification rates. In this case, the classification rate is over 92% with a classifier as fast as applying ten times a threshold. Therefore, using accumulation local moments and boosting techniques we have another fast and highly accurate scheme for real-time or near-real-time tissue characterization.

Once soft and hard plaque are distinguished, we proceed to identify what part of the hard plaque corresponds to calcium. One can argue why not to include a third class in the previous classifier. The reason we prefer not to do so is because experts' identification of calcium plaques is performed by context. Experts use the shadowing produced by the absorption of the echoes, behind a high echo-reflective area, to label a certain area as calcium. In the same way, we take the same approach. On the other hand, the fact of including a third class only hinders the decision process and increases the classifier complexity.

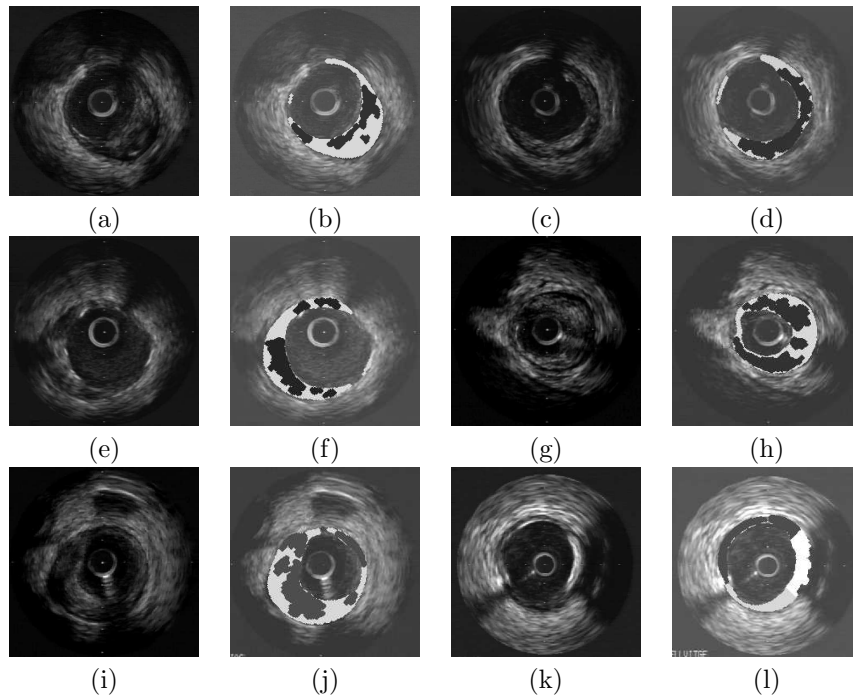


**Figure 6.19:** Tissue characterization results for different patients.

Therefore, the calcium identification process is made by finding the shadowing areas behind hard plaque. Those areas are easily identified because the soft-hard classification also provides this information (figure 6.16) since shadowing areas are classified as non-tissue. We can see a plausible way of finding calcified areas. Figure 6.16.f shows the classification result under the adventitia border of the "hard" tissue. We use one of the previous classified images, the soft-hard classification or the blood-plaque classification. Figure 6.16.g shows in light gray the areas of shadowing, and

therefore, the areas labelled as calcium.

To end the process, the last stage is devoted to recast the resulting classification to its original polar domain by means of a simple coordinate transformation.

Figure 6.19 shows some results of the tissue characterization process. Figures 6.19.a, 6.19.c, 6.19.e, 6.19.g, 6.19.i and 6.19.k, show the original intravascular ultrasound images. Figures 6.19.b, 6.19.d, 6.19.f, 6.19.h, 6.19.j and 6.19.l, show the characterization results (including full automatic intima and adventitia border location). Soft plaque is display in light gray, fibrous plaque is shown in dark gray, and white is used for calcium formations. Regarding the time issues, the full process is performed in 4 seconds using a PIV@3GHz with 1Gb RAM. This time includes the intima and adventitia location as well as tissue characterization. Tissue characterization is performed in less than 0.5 seconds.

At this point, one logical question arises to the reader: How is it possible that the first part of this section stated that co-occurrence matrix measures are the best performing at tissue discrimination and on the second part the author defends the local binary patterns technique? The answer is quite simple. When analyzing the isolated tissues, co-occurrence matrices measures shines because they have high spatial support. As we have shown, texture descriptor with higher local support performs better when deciding if an area is classified as a certain type. On the other hand, local binary patterns and cumulative moments are confined to smaller neighborhoods since they exploit very local features. However, this same reasoning is true for the poorer performance of co-occurrence matrices in accurate intima location and non-isolated tissue. In those scenarios the method tends to overextend its influence by classifying neighboring pixels of a certain area as belonging to majority of the class represented in that area. As a result, though co-occurrence matrices measures have good discriminative power, the comparison in accuracy with the physicians segmentation is degraded due to the response width of the method.



# Chapter 7

## Conclusions and Future lines

This work has shown several tools for pattern recognition in computer vision, ranging from high-level interpretation and classification fusion with *generative snakes*, mathematical techniques involved in the new formulation for geometric deformable models that we have called *Stop and Go* formulation, to pure theoretical classification processes to address semi-supervision and particularization by combining supervised and unsupervised processes in the same framework, *Supervised Clustering Hybrid Competition Scheme*.

We have also attacked the problem of medical image analysis, using classical tools in a first instance and after that designing a new framework for near-real time automatic tissue characterization and IVUS structure analysis.

The following lines detail the conclusions for each of the lines of work described in this document:

1. Generative snakes have been proposed as a tool for integration of the classification and high-level interpretation of the image. This technique relies on the availability of a generative model representing the region of interest and uses this information to create an external energy based on the likelihood map that can be used with suitable modification for guiding a deformable model. In the parametric deformable model context, the modifications include a regularization of the vector field defined by the gradient of the external energy and a two-class likelihood map enhancement. In the geometric context, a topological enhancement of the likelihood map replaces the regularization scheme.

We argue that using the likelihood map instead of a heuristic potential field makes the snake more selective and suitable to the application domain. To this purpose, a texture modelling and a color modelling process has been used to compute the likelihood map. Dimensionality reduction has been applied if necessary to the feature space to make the problem more computationally feasible. In particular, we use Fisher Linear Discriminant Analysis and mixture modelling. The likelihood map is enhanced and its contours are extracted and regularized to assure good performance of the statistic snake. Robustness of our *generative snakes* is shown by means of a wide range of test images from

different domains.

2. We have also introduced a new geodesic snake model *Stop and Go* for a more efficient convergence to shapes. The formulation bases on restricting the regularizing term to the last stages of the snake deformation by decoupling the convergence from the regularity. This decoupling has several advantages over existent geodesic formulations. On one hand, the numeric scheme is more efficient since it admits arbitrary large time increments, except for the last regularizing steps. On the other hand, we build a robust vector field ensuring convergence but, at the same time, snake stabilization. Convergence is achieved by defining separately an dynamic attractive term and an image feature based repulsive one. We also introduce likelihood maps to decouple as well as to define the STOP term of the external potential vector field. By using likelihood maps as an external force the particular version of *Stop and Go* presented in the paper is suited for feature space-based image segmentation (texture, motion, color schemes).

We have compared our scheme to current geometric snakes in terms of computational efficiency and accuracy. The results clearly shows that our method outperforms geodesic snakes in terms of speed of convergence and adaptability to concave regions. Besides, the final models of shapes obtained are smoother than the ones that simple region based scheme yields. Results on real images illustrate the applicability of likelihood maps in different feature spaces.

3. In the classification theory field, a new hybrid technique that combines supervised and unsupervised knowledge has been introduced. This technique exploits the structure of the data set to be classified and adds this constraint to a classical supervised classification based on generative models. In fact, both techniques, supervised and unsupervised, compete to attract each of the test data points.

This work shows how the method can be used to perform semi-supervised classification by setting the labelled data as inputs in the supervised half of the method, while keeping unlabelled data to adapt using the unsupervised half.

*Particularization* has also been addressed. The particularization problem is an emerging problem in some fields that has been very much overlooked by the general classification community. In this sense, we have proposed our technique as an improvement when compared to classical generative classifiers in face of *particularization* problems. We can see that our scheme will have high performance in low dispersion structured coherent test data sets.

We have applied our scheme in two different databases: MNIST and UCI with very promising results. The particularization problem has also been validated using *the writer's test* in the MNIST database.

4. As the last conclusion point, we have used the tools and knowledge provided by the former techniques to address intravascular ultrasound image analysis and tissue characterization. This work is motivated by the necessity of the physicians for studying the vascular diseases using IVUS images. However, this task is complex and suffers from multiple drawbacks (slow manual process subject to

subjectivity interpretation. Therefore, automatic plaque characterization is a highly desirable tool.

Nevertheless, automatic tissue characterization is a problem of high complexity. First of all, it is needed a unique description of the tissues to be classified. This is done by the feature extraction process. In our problem, most of these suitable descriptors are based on texture. Thus, an study of several feature spaces is done, to conclude with some enlightening results. On the other hand, the classification of the feature data is a critical step. Different approaches to the classification problem are described and proposed as candidates in our framework.

At the end, a full segmentation and plaque identification is introduced. As a conclusion, two real-time or near-real-time approaches have been proposed: The first approach combines local binary patterns with maximum likelihood methods. The second approach uses accumulation local moments and boosting techniques.

## 7.1 Future Lines

Much has been done in this work and much still remains to be done in this matters. In particular we recall the following future lines:

1. A better location of boundaries in natural scenes can be useful. In this sense other likelihood map enhancers can be of interest.
2. An exhaustive comparison of the performance of *generative Stop and Go* snakes to the most popular texture and color-based techniques could be of great interest for the community.
3. The SCHCS method is defined for a multidimensional two class problem, the multi-class formulation is still a difficult problem and should be solved.
4. Intravascular image analysis is still an open box of troubles. Though the proposed method alleviates some of them, several still remains. Probably the most notable one is the adventitia border location.
5. Texture based only tissue characterization in IVUS image is a difficult problem. One of the causes lies in the way how the data is obtained. In this sense, access and processing of raw data instead of the processed data displayed in the IVUS image is highly desirable and should be taken into account.



# Bibliography

- [1] Wickline, S., Beyond intravascular imaging: Quantitative ultrasonic tissue characterization of vascular pathology, IEEE Ultrasonics simposium, pp. 1589-1597, 1994.
- [2] Arul, P. and Amin, V., Characterization of beef muscle tissue using texture analysis of ultrasonic images, Proceedings of the Twelfth Southern Biomedical Engineering Conference, pp. 141-143, 1993.
- [3] Mojsilovic, A. and Popovic, M., Analysis and characterization of myocardial tissue with the wavelet image extension [us images], Image Processing, 1995. Proceedings, Vol. 2, pp. 23-26, 1995.
- [4] Jin, X. and Ong, S., Fractal characterization of kidney tissue sections, Engineering in Medicine and Biology Society, 1994. Engineering Advances: New Opportunities for Biomedical Engineers, Proceedings of the 16th Annual International Conference of the IEEE, Vol. 2, pp. 1136-1137, 1994.
- [5] Cohen, F. and Zhu, Q., Quantitative soft-tissue characterization in human organs using texture/attenuation models, Proceedings in Multidimensional Signal Processing Workshop, pp. 47-48, 1989.
- [6] Mavromatis, S. and Boi, J., Medical image segmentation using texture directional features, Engineering in Medicine and Biology Society, 2001. Proceedings of the 23rd Annual International Conference of the IEEE, Vol. 3, pp. 2673-2676, 2001.
- [7] Mavromatis, S., Mammographic mass classification using textural features and descriptive diagnostic data, Digital Signal Processing, 2002. DSP 2002. 2002 14th International Conference on, Vol. 1, pp. 461-464, 2002.
- [8] Donohue, K. and Forsberg, F., Analysis and classification of tissue with scatterer structure templates, Ultrasonics, Ferroelectrics and Frequency Control, IEEE Transactions on, Vol. 46, No. 2, pp. 300-310, 1999.
- [9] Ravizza, P., Myocardial tissue characterization by means of nuclear magnetic resonance imaging, Computers in Cardiology 1991. Proceedings, pp. 501-504, 1991.
- [10] Vandenberg, J., Arterial imaging techniques and tissue characterization using fuzzy logic, Proceedings of the 1994 Second Australian and New Zealand Conference on Intelligent Information Systems, pp. 239-243, 1994.

- [11] Nailon, W. and McLaughlin, S., Comparative study of textural analysis techniques to characterize tissue from intravascular ultrasound, Proc. Of the IEEE International Conference of Image Processing, Switzerland. IEEE Signal Processing Society:USA, pp. 303-305, 1996.
- [12] Nailon, W. and McLaughlin, S., Intravascular ultrasound image interpretation, Proc. Of the International Conference on Pattern Recognition, Austria. IEEE Computer Society Press:USA, pp. 503-506, 1996.
- [13] Nailon, W., Fractal texture analysis: An aid to tissue characterization with intravascular ultrasound, Proceedings 19th International Conference - IEEE/EMBS, pp. 534-537, 1997.
- [14] Spencer, T., Characterization of atherosclerotic plaque by spectral analysis of 30mhz intravascular ultrasound radio frequency data, IEEE Ultrasonics symposium, pp. 1073-1076, 1996.
- [15] Dixon, K., Characterization of coronary plaque in intravascular ultrasound using histological correlation, 19th International Conference-IEEE/EMBS, pp. 530-533, 1997.
- [16] Ahmed, M. and Leyman, A., Tissue characterization using radial transform and higher order statistics, Nordic Signal Processing Symposium, pp. 13-16, 2000.
- [17] de Korte, C. L. and van der Steen, A. F. W., Identification of atherosclerotic plaque components with intravascular ultrasound elastography in vivo: a yucatan pig study, Circulation, Vol. 105, No. 14, pp. 1627-1630, 2002.
- [18] Zhang, X. and Sonka, M., Tissue characterization in intravascular ultrasound images, IEEE Transactions on Medical Imaging, Vol. 17, No. 6, pp. 889-899, 1998.
- [19] Pujol, O. and Radeva, P., Automatic segmentation of lumen in intravascular ultrasound images: An evaluation of texture feature extractors, Proceedings for IBERAMIA 2002, pp. 159-168, 2002.
- [20] Pujol, O. and Radeva, P., Near real time plaque segmentation of ivus, Proceedings of Computers in Cardiology, pp. 159-168, 2003.
- [21] Randen, T. and Husoy, J. H., Filtering for texture classification: A comparative study, Pattern Recognition, Vol. 21, No. 4, pp. 291-310, 1999.
- [22] Haralick, R., Shanmugam, K. and Dinstein, I., Textural features for image classification, IEEE Trans. System, Man, Cybernetics, Vol. 3, pp. 610-621, 1973.
- [23] Tuceryan, M., Moment based texture segmentation, Pattern Recognition Letters, Vol. 15, pp. 659-668, 1994.
- [24] Lindeberg, T., Scale-Space Theory in Computer Vision, Kluwer Academic Publishers, 1994.

- [25] Jain, A. and Farrokhnia, F., Unsupervised texture segmentation using gabor filters, *Systems, Man and Cybernetics*, 1990. Conference Proceedings, pp. 14-19, 1990.
- [26] Mallat, S., A theory for multiresolution signal decomposition: The wavelet representation, *IEEE Transactions on Pattern Analysis and Machine Intelligence*, Vol. 11, No. 7, pp. 674-694, 1989.
- [27] Mandelbrot, B., *The Fractal Geometry of Nature*, W H Freeman and Co. New York, 1983.
- [28] Ojala, T., Pietikainen, M. and Maenpaa, T., Multiresolution gray-scale and rotation invariant texture classification with local binary patterns, *IEEE Transactions on Pattern Analysis and Machine Intelligence*, Vol. 24, No. 7, pp. 971-987, 2002.
- [29] Julesz, B., Visual pattern discrimination, *IRE Transactions on Information Theory*, Vol. IT-8, pp. 84-92, 1962.
- [30] Ohanian, P. and Dubes, R., Performance evaluation for four classes of textural features, *Pattern Recognition*, Vol. 25, No. 8, pp. 819-833, 1992.
- [31] Martinez, J. and Thomas, F., Efficient computation of local geometric moments, *IEEE Trans. Image Processing*, Vol. 11, No. 9, pp. 1102-1111, 2002
- [32] Caelli, T. and Oguztoreli, M. N., Some tasks and signal dependent rules for spatial vision, *Spatial Vision*, No. 2, pp. 295-315, 1987.
- [33] Chaudhuri, B. and Sarkar, N., Texture segmentation using fractal dimension, *IEEE Transactions on Pattern Analysis and Machine Intelligence*, Vol. 17, No. 1, pp. 72-77, 1995.
- [34] Lindeberg, T., Scale-space theory: A basic tool for analysing structures at different scales, *Journal of Applied Statistics*, Vol. 21, No. 2, pp. 225-270, 1994.
- [35] Rao, R. and Ballard, D., Natural basis functions and topographic memory for face recognition, *Proceedings of International Joint Conference on Artificial Intelligence*, pp. 10-17, 1995.
- [36] Lumbreras, F., PhD Thesis: Segmentation, Classification and Modelization of Textures by means of Multiresolution Descomposition Techniques, CVC, UAB, 2001.
- [37] Jain, A. and Farrokhnia, F., A multi-channel filtering approach to texture segmentation, *Computer Vision and Pattern Recognition*, 1991. Proceedings CVPR '91, pp. 364-370, 1991.
- [38] Fukunaga, K., *Introduction to statistical pattern recognition*, Academic Press, 1971.
- [39] Duda, R. and Hart, P., *Pattern Classification*, Wiley-Interscience, 2001. Second Edition.

- [40] Belhumeur, P., Eigenfaces vs fisherfaces: Recognition using class specific linear projection, *IEEE Pattern Analysis and Machine Intelligence*, Vol. 19, No. 7, pp. 711-720, 1997.
- [41] Schapire, R. E., The boosting approach to machine learning. an overview, MSRI Workshop on Nonlinear Estimation and Classification, 2002.
- [42] Viola, P. and Jones, M., Rapid object detection using a boosted cascade of simple features, *Conference on Computer Vision and Pattern Recognition*, p. 511-518, 2001.
- [43] Sonka, M. and Zhang, X., Segmentation of intravascular ultrasound images: A knowledge-based approach, *IEEE Transactions on Medical Imaging*, Vol. 17, No. 6, pp. 889-899, 1998.
- [44] von Birgelen, C., Computerized assessment of coronary lumen and atherosclerotic plaque dimensions in three-dimensional intravascular ultrasound correlated with histomorphometry, *Amer. J. Cardiology*, Vol. 78, pp. 1202-1209, 1996.
- [45] Klingensmith, J., Shekhar, R., and Vince, D., Evaluation of three-dimensional segmentation algorithms for identification of luminal and medial-adventitial borders in intravascular ultrasound images, *IEEE Trans. on Medical Imaging*, Vol. 19, No. 10, pp. 996-1011, 2000.
- [46] McInerney, T. and Terzopoulos, D., Deformable models in medical images analysis: a survey, *Medical Image Analysis*, Vol. 1, No. 2, pp. 91-108, 1996.
- [47] Nair A., Obuchowski N., Classification of Atherosclerotic Plaque Composition by Spectral Analysis of Intravascular Ultrasound Data. *IEEE Ultrasonics symposium 2001*, pp. 1569-1572, 2001.
- [48] Nair A., Kuban D., Assessing spectral algorithms to predict atherosclerotic plaque composition with normalized and raw intravascular ultrasound data, *Ultrasound in Med. Bio.*, Vol. 27, pp. 1319-1331, 2001.
- [49] Nair A., Kuban D., Coronary Plaque Classification with Intravascular Ultrasound Radiofrequency Data Analysis, *Circulation*, Vol. 106, pp. 2200-2206, 2002.
- [50] Pujol, O. and Rosales, M. and Radeva, P., Intravascular Ultrasound Images Vessel Characterization using AdaBoost, *Functional Imaging and Modelling of the Heart. Lecture Notes on Computer Science 2674*, pp. 242-251, 2003.
- [51] V. Caselles, F. Catte, T. Coll, and F. Dibos. A geometric model for actives contours. *Numerische Mathematik*, 66:1-31, 1993.
- [52] B. Chaudhuri, N. Sarkar. Texture segmentation using fractal dimension. *IEEE Transactions on Pattern Analysis and Machine Intelligence* 17(1):72-77,1995
- [53] L. D. Cohen. On active contour models and ballons. *CVGIP:Image understanding*, 53(2):211-218, 1991.



- [54] T.F. Cootes, G.J. Edwards, C.J Taylor. Active appearance models. *IEEE Transactions on Pattern Analysis and Machine Intelligence* 23(6):681-685,2001.
- [55] H. Delingette and J. Montagnat. Shape and Topology Constraints on Parametric Active Contours. *Computer Vision and Image Understanding: CVIU* 83(2):140-171,2001.
- [56] R. O. Duda, Peter E. Hart, David G. Stork. *Pattern Classification*. Wiley-Interscience,2001. 2nd Ed.
- [57] R. Haralick and K. Shanmugam and I. Dinstein. Textural Features for Image Classification *IEEE Trans. System, Man, Cybernetics*,3,610-621. 1973
- [58] T. Hofmann, J. Puzicha, and J.M. Buhmann. Unsupervised Texture Segmentation in a Deterministic Annealing Framework. *IEEE Transactions on Pattern Analysis and Machine Intelligence*, 20(8):803-818,1998.
- [59] A. Jain, F. Farrokhnia. Unsupervised texture segmentation using Gabor Filters. *IEEE Pattern Recognition* 24(12):1167-1186, 1991.
- [60] B. Julesz. Visual Pattern Discrimination. *IRE Transactions on Information Theory* IT-8:84-92,1962.
- [61] M. Kass, A. Witkin, and D. Terzopoulos. Snakes, Active contour models. *Int. J. Computer Vision*, 1(4):321-331, 1987.
- [62] A. Laine, J. Fan. Frame representations for texture segmentation. *IEEE Transactions on Image Processing* 5(5):771-779,1996.
- [63] J. Malik, S. Belongie, T. Leung and J. Shi. Contour and Texture Analysis for Image Segmentation. *International Journal of Computer Vision* 43(1),7-27,2001.
- [64] J. Malik and P. Perona. A Computational Model of Texture Segmentation. *In IEEE Conference on Computer Vision and Pattern Recognition*, pp.326-332,1989.
- [65] S. G. Mallat. A Theory for Multiresolution Signal Decomposition. San Diego, Calif.: Academic Press, 1992.
- [66] B. Manjunath, R. Chellapa. Unsupervised Texture Segmentation using Markov Random Field Models. *IEEE Transactions on Pattern Analysis and Machine Intelligence*, 13:478-482.1991.
- [67] J. Mao, A. Jain. Texture Classification and segmentation using multiresolution simultaneous autoregressive models. *Pattern Recognition* 25:173-188,1992.
- [68] T. McInerney and D. Terzopoulos. Deformable models in medical images analysis: a survey. *Medical Image Analysis*, 1(2):91-108, 1996.
- [69] T. McInerney and D. Terzopoulos. T-Snakes: Topology Adaptive Snakes. *Medical Image Analysis*, 4:73-91, 2000.

- [70] P.P. Ohanian and R.C. Dubes. Performance Evaluation for Four Classes of Textural Features. *Pattern Recognition*,25(8),819-833, 1992.
- [71] N. Paragios, R. Deriche. Geodesic Active Contours for Supervised Texture Segmentation. *Proc. of Computer Vision and Pattern Recognition 2*,422-427, 1999.
- [72] N. Paragios, R. Deriche. Unifying Boundary and Region-based Information for Geodesic Active Tracking. *Proceedings of Computer Vision and Pattern Recognition 2*:300-305.1999.
- [73] J. Prince and C. Xu.A new external force model for snakes.*1996 Image and Multidimensional Signal Processing Workshop*, pp 30-31,1996.
- [74] J. Puzicha and T. Hofmann and J. Buhmann.Non-parametric similarity measures for unsupervised texture segmentation and image retrieval. *In Proceedings of the Conference on Computer Vision and Pattern Recognition*,1997
- [75] P. Radeva and J. Vitrià. Discriminant Snakes for Region-Based Segmentation.*Proceedings of ICIP*, Thessaloniki, Greece, October, 2001
- [76] T. Randen and J. H. Husoy. Filtering for Texture Classification: A Comparative Study. *Pattern Recognition* 21(4),291-310.1999.
- [77] M. Sonka, X. Zhang, M. Siebes. Segmentation of Intravascular Ultrasound Images: A knowledge-based Approach. *IEEE Transactions on Medical Imaging* 14(4):719-732, 1995.
- [78] R. Szeliski. Bayesian modeling of uncertainty in low-level vision. *International Journal of Computer Vision* 5:271-301, 1990.
- [79] D. Terzopoulos and R. Szeliski. Tracking with Kalman snakes. In A. Blake, A. Yuille,eds. *Active Vision*. Cambridge. MA:MIT Press 3-20.
- [80] C. Xu, J. L. Prince. Generalized gradient vector flow external forces for active contours. *Signal Processing*, 71:131-139, 1998.
- [81] C. Xu, J. L. Prince. Gradient Vector Flow: A new external force for snakes. *IEEE Proc. Conf. on Comp. Vis. Patt. Recog. (CVPR'97)*, 66-71, 1997.
- [82] S. C. Zhu. Region Competition: Unifying Snakes, Region Growing, and Bayes/MDL for Multi-band Image Segmentation. Harwad Robotics Lab. Technical Report no. 94-10.
- [83] L.C. Evans. *Partial Differential equations*. Berkeley Mathematics Lecture Notes, vol. 3B, 1993.
- [84] D. Gil, and P. Radeva, *Curvature Vector Flow to Assure Convergent Deformable Models*. EMMCVF'03.
- [85] S. Jehan-Besson, M. Barlaud, and G. Aubert, *DREAM'S: Deformable Regions driven by an Eulerian Accurate Minimization Method for image and video Segmentation* Submitted to Int. Jour. of Computer Vision, 2003.

- [86] S. Osher and J. A. Sethian, *Fronts propagating with curvature-dependent speed: algorithms based on Hamilton-Jacobi formulations*, J. Comp. Phys. 79, pp.12-49, 1988.
- [87] O. Pujol, and P. Radeva, *Texture Segmentation by Statistic Deformable Models*, Int. Journal of Image and Graphics, (accepted, pending publication).
- [88] R. Ronfard, *Region-based strategies for active contour models*, Int. Jour. of Computer Vision, 13(2) pp. 229-251.
- [89] C. Samson, L. Blanc-Féraud, G. Aubert, and J. Zerubia, *A level set model for image classification*. Proc. of Scale-Space Th. in Comp. Vis., pp.26-27, Sept. 1999.
- [90] G. Sapiro, *Color snakes*. Comp. Vis. and Im. Und. , 68:2 pp.247-253, 1997.
- [91] A. Tveito, R. Winther. *Introduction to Partial Differential Equations*. Texts in applied Math., n 29, Springer-Verlag, 1998.
- [92] A. Yezzi, A. Tsai, and A. Willsky, *A statistical approach to snakes for bimodal and trimodal imagery*, Int. Conf. on Image Processing. Kobe (Japan), 1999.
- [93] C.Xu and J.L. Prince, *Generalized gradient vector flow external forces for active contours*. Sig. Proc., An Intern. Journal, 71(2), pp. 132-139, 1998.
- [94] C. Xu, A. Yezzi, and J. Prince, *On the Relationship between Parametric and Geometric Active Contours*. Proc. of 34th Asilomar Conf. on Sig., Sys. and Comp., pp. 483-489, Oct., 2000.
- [95] A. Chakraborty, L. Staib, and J. Duncan, *Deformable boundary finding in medical images by integrating gradient and region information*, IEEE Trans. on Medical Imaging, 15, pp. 859-870, 1996.
- [96] P. Salembier, A. Oliveras and L. Garrido, *Antiextensive Connected Operators for Image and Sequence Processing*, IEEE Trans. on Image Processing, vol.7 No 4, April, 1998.
- [97] Miin-Shen Yang and Kuo-Lung Wu, *A Similarity-Based Robust Clustering Method*. IEEE Trans. on PAMI, Vol. 26, No. 4, pp. 434-448, 2004.
- [98] J.C. Bezdek. *Pattern Recognition with Fuzzy Objectiv Function Algorithm*. Plenum Press, 1981.
- [99] J.C. Bezdek. *Cluster Validity with Fuzzy Sets*. J. Cybernetics, vol.3, pp. 58-73, 1974.
- [100] R.N. Dave and R. Krishnapuram. *Robust Clustering Methods: A Unified View*. IEEE Trans. Fuzzy Systems, vol. 5, pp. 270-293, 1997.
- [101] D.L. Davies and D.W. Bouldin. *A Cluster Separation Measure*. IEEE Trans. on PAMI, vol. 1, pp. 224-227, 1979.

- [102] R.O. Duda and P.E. Hart. Pattern Classification and Scene Analysis. Wiley, 1973.
- [103] S. Grossberg. Adaptive Pattern Classification and Universal Recoding, I: Parallel Development and Coding of Neural Features Detectors. *Biological Cybernetics*, vol. 23, pp. 121-134, 1976.
- [104] E.E. Gustafson and W.C. Kessel. Fuzzy Clustering with a Fuzzy Matrix. *Proc. IEEE Conf. Design and Control*, pp. 761-766, 1979.
- [105] J.A. Hartigan. Clustering Algorithms. Wiley, 1975.
- [106] P.J. Huber. Robust Statistics. Wiley, 1981.
- [107] A.K. Jain and J. Mao. Statistical Pattern Recognition: A Review. *IEEE on PAMI*, vol. 22, pp. 4-37, 2000.
- [108] L. Kaufman and P.J. Rousseeuw. Finding Groups in Data: An Introduction to Cluster Analysis. Wiley, 1990.
- [109] T. Kohonen. Learning Vector Quantization. *Neural Network*, vol. 1, pp. 303, 1988.
- [110] R. Krishnapuram and O. Masraoui. Fuzzy and Probabilistic Shell Clustering Algorithm and Their Applications to Boundary Detection and Surface Approximation. *IEEE Trans on Fuzzy Systems*, vol. 3, pp. 29-60, 1995.
- [111] R.P. Lippmann. An Introduction to Computing with Neural Nets. *IEEE ASSP Magazine*, pp. 4-22, Apr. 1987.
- [112] N.R. Pal and J.C. Bezdek. On Cluster Validity for Fuzzy c-Means Model. *IEEE Trans. on Fuzzy Systems*, vol. 1, pp. 370-379, 1995.
- [113] G.J. McLachlan and T. Krishnan. The EM Algorithm and Extensions. John Wiley and Sons, 1997.
- [114] F.J. McLachlan and K.E. Basford. Mixture Models: Inference and Applications to Clustering. New York: Marcel Dekker, 1988.
- [115] E.C.K. Tsao and N.R. Pal. Fuzzy Kohonen Clustering Net Works. *Pattern Recognition*, vol. 27, pp. 757-764, 1994.
- [116] K.L. Wu and M.S. Yang. Alternative c-Means Clustering Algorithms. *Pattern Recognition*, vol. 35, pp. 2267-2278, 2002.
- [117] X.L. Xie and G. Beni. A Validity Measure for Fuzzy Clustering. *IEEE Trans on PAMI*, vol. 13, pp.841-847, 1991.
- [118] A. McCallum and K. Nigam. Employing EM and pool-based active learning for text classification. *Int. Conf. on Machine Learning*, pp. 359-367, 1998.
- [119] T.J. O'Neill. Normal Discrimination with unclassified observations. *J. of American Statistical Assoc.*, vol. 73, pp. 821-826, 1978.

- [120] F. Gagliardi and M. Cirelo. Semi-Supervised Learning of Mixture Models. Proc. XXth ICML, 2003.
- [121] A. Blum and T. Mitchell. Combining labeled and unlabeled data with co-training. Proc. XIth. Annual Conference on Computational Learning Theory, Madison, WI, 1998.
- [122] T. Joachims. Transductive inference for text classification using support vector machines. Proc. XVIth ICML, Bled, Slovenia, 1999.
- [123] K. Nigam, A.K. McCallum, S. Thrun and T. Mitchell. Text classification from labeled and unlabeled documents using EM. Machine Learning, vol. 39, pp. 103-134, 2000.
- [124] S. Basu, A. Banerjee and R.J. Mooney. Semi-supervised clustering by seeding. Proc. XIXth ICML, pp. 19-26, 2002.
- [125] E.P. Xing, A.Y. Ng, M.I. Jordan and S. Russell. Distance Metric Learning, with applications to clustering with side-information. Advances in Neural Information Processing Systems 15. MIT Press, 2003.
- [126] A. Demiriz, K.P. Bennett and M.J. Embrechts. Semi-supervised clustering using genetic algorithms. ANNIE'99, 1999.
- [127] K. Wangstaff, C. Cardie, S. Rogers and S. Schroedl. Constrained K-Means clustering with background knowledge. Proc. XVIIIth ICML, 2001.
- [128] J. Sinkkonen and S. Kaski. Semisupervised clustering based on conditional distributions in an auxiliary space. Tech. rep. A60, Helsinki Univ. of Technology, 2000.
- [129] M. Bilenko and R.J. Mooney. Adaptive duplicate detection using learnable string similarity measures. Proc. 9th ACM SIGKDD Int. Conf. on Knowledge Discovery and Data Mining, pp. 39-48, 2003.
- [130] D. Cohn, R. Caruana and A. McCallum. Semi-supervised clustering with user feedback. Unpublished. 2000. Available at <http://www-2.cs.cmu.edu/mccallum/> and attached to this work.
- [131] D. Klein, S.D. Kamvar and C. Manning. From instance-level constraints to space-level constraints: Making the most of prior knowledge in data clustering. Proc. XIXth ICML, Sydney, Australia, 2002.
- [132] A.B. Hillel, T. Hertz, N. Shental and D. Weinshall. Learning distance functions using equivalence relations. Proc. ICML, 2003.
- [133] W.J. Clancey. A Tutorial on Situated Learning. In Proc. of the International Conference on Computers and Education, pp. 49-70, 1995.
- [134] L. Reder and R.L. Klatzky. The effect of Context on Training: Is Learning Situated? , Tech Reprt CMU-CS-94-187 and CMU-HCIL-94-108, School of Computer Science, Carnegie Mellon University, 1994.

- [135] D. Druckman and R.A. Bjork. Transfer: Training for Performance. Learning, Remembering, Believing: Enhancing Human Performance, pp.25-56. Washington DC, National Academy Press, 1994.
- [136] A.R. Coden, S.V. Pakhamov and C.G. Chute. Domain-Specific Language Models and Lexicons for Tagging. Tech. Reprt. RC23195 (W0404-146) IBM Research Division, 2004.
- [137] P.R. Clarkson and A.J. Robinson. Language Model Adaptation using mixtures and an exponentially decaying Cache. Proc ICASSP, 1997.
- [138] M. Federico. Bayesian Estimation Methods for N-Gram Language Model Adaptation. The IVth Int Conf on Spoken Language Processing, ICSLP, 1996.
- [139] S. Kumar, A. Loui and M. Herbert. An observation-constrained generative approach for probabilistic classification of image regions. Image and Vision Computing, vol. 21, pp. 87-97, 2003.
- [140] C.L. Blake and C.J. Merz. UCI Repository of machine learning databases. <http://www.ics.uci.edu/~mllearn/MLRepository.html>. 1998.

# List of Publications

## Book Chapters

- O. Pujol and P. Radeva. *Supervised Texture Classification for Intravascular Tissue Characterization*. Handbook of Medical Imaging. Editorial: Kluwer Academic/ Plenum Publishers, NY, USA, 2004. (In Press)
- O. Pujol and P. Radeva. *On the assessment of texture descriptors in intravascular ultrasound images: A boosting approach to a feasible plaque classification*. Plaque Imaging. Editorial: Kluwer Academic/ Plenum Publishers, NY, USA, 2004. (In Press)

## Journals

- O. Pujol, D. Gil, P. Radeva. *Fundamentals of Stop and Go Active Models*, Journal of Image and Vision Understanding.(Submitted 8/7/2003)
- O. Pujol, P. Radeva. *Supervised Clustering Hybrid Competition Scheme*, IEEE Pattern Analysis and Machine Intelligence.(Submitted 8/7/2004)
- O. Pujol, P. Radeva. *Automatic framework for tissue characterization in IVUS images*, IEEE Medical Imaging.(Submitted 8/7/2004)
- O. Pujol, P. Radeva. *Texture Segmentation by Statistic Deformable Models* , International Journal of Image and Graphics, vol.4 (3), 2003. (in press).

## Lecture Notes and other conference proceedings

- O. Pujol, P. Radeva, J. Vitria, J. Mauri. *Adaboost to classify plaque appearance in IVUS images*. Lecture Notes in Computer Science (CIARP'2004) (In Press).
- M. Rosales, O. Pujol, P. Radeva. *Simulation Model of Intravascular Ultrasound Images*. Lecture Notes in Computer Science (MICCAI,04) (In Press).
- O. Pujol, M. Rosales, P. Radeva. *Intravascular Ultrasound Images Vessel Characterization using AdaBoost*, Functional Imaging and Modelling of the Heart: Lecture Notes on Computer Science 2674, pp.242-251, 2003. ISBN: 3-540-40262-4.

- D. Rotger, M. Rosales, J. Garca, O. Pujol, J. Mauri, P. Radeva, *ActiveVessel: A New Multimedia Workstation for IVUS and Angiography Fusion*, Proceedings of Computers in Cardiology, Thessaloniki, Greece, September, 2003 (in press).
- O. Pujol, D. Rotger, P. Radeva, O. Rodriguez, J. Mauri, *Near Real Time Plaque Segmentation of IVUS*, Proceedings of Computers in Cardiology, Thessaloniki, Greece, September, 2003 (in press).
- O. Rodriguez Leor, E. Fernandez Nofrerias, J. Mauri, C. Garcia Garcia, R. Villuendas, V. Valle Tudela, O. Pujol, P. Radeva, *Intravascular ultrasound segmentation using local binary patterns*, European Heart Journal, ESC Congress 2003, Vienna, Austria, 2003.
- O. Rodriguez, J. Mauri, E. Fernandez-Nofrerias, A. Tovar, R. Villuendas, V. Valle, O. Pujol, P. Radeva, *Anlisis de Texturas mediante la Modificacin de un Modelo Binario Local para la Segmentacin Automtica de Secuencias de Ecografa Intracoronaria*, Revista Espaola de Cardiologa, 56(2), Congreso de las Enfermedades Cardiovasculares, Sevilla, Spain, Octubre, 2003.
- Oriol Pujol and Petia Radeva, *Lumen detection in ivus images using snakes in a statistical framework*, XX Congreso Anual de la Sociedad Espaola de Ingeniera Biomdica, Zaragoza, Noviembre, 2002.
- O. Pujol, P. Radeva, J. Mauri and E. Nofrerias, *Automatic segmentation of lumen in Intravascular Ultrasound Images: An evaluation of texture feature extractors*, Iberamia, 2002, Springer-Verlag.
- Gmez, Mauri, Fernandez-Nofrerias, Rodriguez-Leor, Diego, Juli, Pujol, Radeva, *Diferenciacin de las estructuras del vaso coronario mediante el procesamiento de imgenes y el anlisis de las diferentes texturas a partir de la ecografa intracoronaria* (N 848), XXXVIII Congreso Nacional de la Sociedad Espaola de Cardiologa, Madrid, 16- 19 October, 2002.
- E. F. Nofrerias, J. Mauri, J. Comn, B. Garca del Blasco, E. Irculis, J. A. Gmez Hospital, P. Valdovinos, F. Jara, A. Cequier, E. Esplugas, C. Caero, O. Pujol, D. Gil, R. Radeva, R. Toledo, J. Villanueva. *Selecci de l'Stent en base a la Longitud Real de la Lesi: l'Entorn Informtic*. Revista de la Societat Catalana de Cardiologia. Barcelona, Juny de 2000.
- J. Mauri, E. F. Nofrerias, B. Garca del Blasco, E. Irculis, J. A. Gmez Hospital, J. Comn, M. A. Snchez Corral, F. Jara, , A. Cequier, E. Esplugas, D. Gil, O. Pujol, C. Caero, R. Radeva, R. Toledo, J. Villanueva. *Moviment del Vas en l'Anlisi de les Imatges d'Ecografia Intracoronria: un Model Matemtic*. Revista de la Societat Catalana de Cardiologia. Barcelona, Juny de 2000.
- J. Mauri, E. F. Nofrerias, J. Comn, B. Garca del Blasco, E. Irculis, J. A. Gmez Hospital, P. Valdovinos, F. Jara, A. Cequier, E. Esplugas, O. Pujol, C. Caero, D. Gil, R. Radeva, R. Toledo, J. Villanueva. *Avaluaci del Conjunt Stent/Artria mitjanant Ecografia Intracoronria: L'Entorn Informtic*. Revista de la Societat Catalana de Cardiologia. Barcelona, Juny de 2000.



- O. Pujol, Model Based 3D-Interpolation of IVUS Images, Computer Vision Center. Technical Report 27. September 1999.
- C. Caero, P. Radeva, O. Pujol, R. Toledo, D. Gil, J. Saludes, J. J. Villanueva, B. Garcia del Blanco, J. Mauri, E. F. Nofreras, J. A. Gmez-Hospital, E. Irculis, J. Comn, C. Quiles, F. Jara, A. Cequier, E. Esplugas, *Optimal Stent Implantation: Three-dimensional Evaluation of the Mutual Position of Stent and Vessel via Intracoronary Ecography*, Proceedings of International Conference on Computer in Cardiology (CIC'99), Hannover, 1999.
- O. Pujol, P. Radeva, C. Caero, R. Toledo, D. Gil, J. Saludes, J. J. Villanueva, B. Garca del Blanco, J. Mauri, E. F. Nofreras, J. A. Gmez-Hospital, E. Irculis, J. Comn, C. Quiles, F. Jara, A. Cequier, E. Esplugas, *Three-dimensional reconstruction and quantification of the coronary tree using intravascular ultrasound images*, Proceedings of International Conference on Computer in Cardiology (CIC'99), Hannover, 1999
- E Irculis, J Mauri , B Garca del Blanco, E F Nofreras, JA Gomez Hospital, J Comn, C Quiles, F Jara, A Cequier, E Esplugas. O Pujol, P Radeva, R Toledo, J Villanueva,. *Reconstrucci tridimensional i quantificaci de l'arbre coronari utilitzant ecografia intracoronria*, Catalanian Conference on Cardiology, Sagar, Girona, 1999.
- B Garcia del Blanco , J Mauri , E F-Nofreras, J.A Gmez-Hospital, E Irculis, J Comn, C Quiles, F Jara, A Cequier, E Esplugas, O Pujol, C Caero, P Radeva, R Toledo, J Villanueva, *Implantaci ptima d'stents: Avaluaci tridimensional del conjunt stent/artria mitjanant ecografia intracoronria*, Catalanian Conference on Cardiology, Sagar, Girona, 1999.